

# UC Davis

## UC Davis Previously Published Works

### Title

Structure in the event-by-event energy-dependent neutron- $\gamma$  multiplicity correlations in Cf252(sf)

### Permalink

<https://escholarship.org/uc/item/0nj5n8tt>

### Journal

Physical Review C, 104(2)

### ISSN

2469-9985

### Authors

Marin, Stefano

Okar, M Stephan

Sansevero, Eoin P

et al.

### Publication Date









2021-08-01

### DOI

10.1103/physrevc.104.024602

Peer reviewed

# Structure in the event-by-event energy-dependent neutron- $\gamma$ multiplicity correlations in $^{252}\text{Cf}(\text{sf})$

Stefano Marin <sup>1,\*</sup>, M. Stephan Okar,<sup>1</sup> Eoin P. Sansevero,<sup>1</sup> Isabel E. Hernandez <sup>1</sup>, Catherine A. Ballard <sup>1</sup>,  
Ramona Vogt <sup>2,3</sup>, Jørgen Randrup,<sup>4</sup> Patrick Talou <sup>5</sup>, Amy E. Lovell <sup>6</sup>, Ionel Stetcu,<sup>6</sup> Olivier Serot,<sup>7</sup> Olivier Litaize <sup>7</sup>,  
Abdelhazize Chebboubi <sup>7</sup>, Shaun D. Clarke,<sup>1</sup> Vladimir A. Protopopescu,<sup>8</sup> and Sara A. Pozzi<sup>1,9</sup>

<sup>1</sup>*Department of Nuclear Engineering and Radiological Sciences, University of Michigan, Ann Arbor, Michigan 48109, USA*

<sup>2</sup>*Nuclear and Chemical Sciences Division, Lawrence Livermore National Laboratory, Livermore, California 94550, USA*

<sup>3</sup>*Department of Physics and Astronomy Department, University of California, Davis, California 95616, USA*

<sup>4</sup>*Nuclear Science Division, Lawrence Berkeley National Laboratory, Berkeley, California 94720, USA*

<sup>5</sup>*Computational Physics Division, Los Alamos National Laboratory, Los Alamos, New Mexico 87545, USA*

<sup>6</sup>*Theoretical Physics Division, Los Alamos National Laboratory, Los Alamos, New Mexico 87545, USA*

<sup>7</sup>*CEA, DES, IRESNE, DER, SPRC, Physics Studies Laboratory, Cadarache, F-13108 Saint-Paul-lès-Durance, France*

<sup>8</sup>*Oak Ridge National Laboratory, Oak Ridge, Tennessee 37830, USA*

<sup>9</sup>*Department of Physics, University of Michigan, Ann Arbor, Michigan 48109, USA*

The emission of neutrons and  $\gamma$  rays by fission fragments reveal important information about the properties of fragments immediately following scission. The initial fragment properties, correlations between fragments, and emission competition give rise to correlations in neutron- $\gamma$  emission. Recent theoretical and experimental advances have been proposed to explain the mechanism of angular momentum generation in fission, which would result in observable signature in neutron- $\gamma$  emission correlations. In this paper, we present a novel analysis method of neutrons and  $\gamma$  rays emitted by fission fragments that allows us to discern structure in the observed correlations. We have analyzed data collected on  $^{252}\text{Cf}(\text{sf})$  at the Chi-Nu array at the Los Alamos Neutron Science Center. Through our analysis of the energy-differential neutron- $\gamma$  multiplicity covariance, we have observed enhanced neutron- $\gamma$  correlations, corresponding to rotational band  $\gamma$ -ray transitions, at  $\gamma$ -ray energies of 0.7 and 1.2 MeV. To shed light on the origin of this structure, we compare the experimental data with the predictions of three model calculations. The origin of the observed correlation structure is understood in terms of a positive spin-energy correlation in the generation of angular momentum in fission.

## I. INTRODUCTION

Heavy atomic nuclei can decay by fission, i.e., separating into two or more large nuclear fragments. The complexities of the strong nuclear forces and the electromagnetic interactions between hundreds of nucleons lead to a variety of exit channels for the fission process, resulting in stochastic distributions of both masses and kinetic energies of the produced fission fragment [1]. Large correlated variations exist also in the excitation energies and angular momenta of the fragments [2–4], as well as in the emission of neutrons and  $\gamma$  rays [5]. The initial conditions of fission fragments cannot be directly probed due in part to the short time scales of fragment de-excitation. To study the condition of the fragments immediately after scission, we study the emission of neutrons and  $\gamma$  rays, since their emission is highly correlated with the initial fragment conditions [2,6]. Particularly important open questions in fission modeling are the generation of angular momentum at scission [3,7,8] and the sharing of excitation energy between fragments [4,9].

In a previous publication [10], we surveyed the results of several earlier publications on event-by-event neutron- $\gamma$  multiplicity correlations in  $^{252}\text{Cf}(\text{sf})$ . After developing and applying analytic unfolding techniques to the experimental data, we found these data to be in qualitative agreement with one another and with the predictions of model calculations. Specifically, the results indicate the existence of significant negative event-by-event correlations between the neutron- $\gamma$  multiplicities. However, these experimental results were affected by energy-dependent systematic biases.

The goal of this paper is to further develop our previous analysis of neutron- $\gamma$  correlations by studying energy-dependent correlations in the spontaneous fission of  $^{252}\text{Cf}$ . We find that the structure of the correlations observed in the experiment can be explained by known and predicted physical mechanisms and indicates the existence of an energy-dependence in the generation of angular momentum in fission.

Section II presents a brief overview of the physical mechanisms that give rise to correlations in fission. Section III presents the mathematical formalism required to extract and quantify the predicted correlations. Section IV reports the experimental setup and the techniques used in experiment. In Sec. V, we describe the most prominent features of the

---

\*stmarin@umich.edu

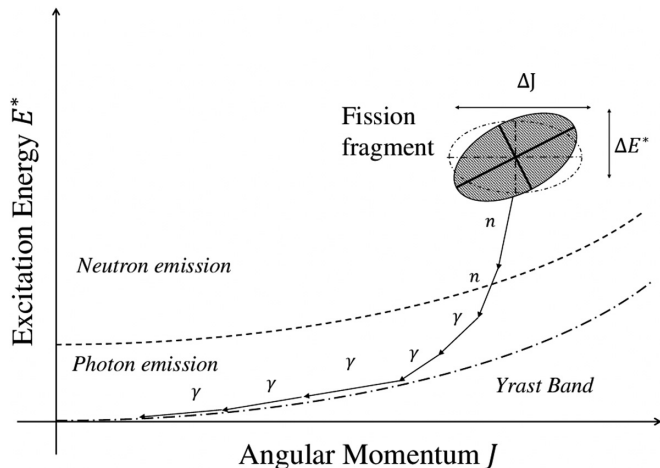


FIG. 1. Schematic representation of neutron and  $\gamma$ -ray emission from fission fragments. The neutron separation energy is indicated by a dashed line, and the yrast rotational band is indicated as a dot-dashed line [12].

neutron- $\gamma$  correlations and compare them with model calculations. Lastly, in Sec. VI, we draw our conclusions on the origin of the observed correlations.

## II. SOURCES OF CORRELATIONS

### A. Neutron and $\gamma$ -ray emission

Following scission, fission fragments promptly decay by neutron emission, if energetically possible, followed by  $\gamma$ -ray emission. Two modes of  $\gamma$ -ray emission are usually distinguished [5,11]: statistical  $\gamma$  rays in the continuum at higher intrinsic excitation energies (STAT), and band-transition  $\gamma$  rays in the discrete-level region (DISC). A pictorial diagram, inspired by Ref. [11], is shown in Fig. 1. We have explicitly drawn a tilted initial distribution of the initial fragment conditions to highlight suspected spin-energy correlations in the formation of fission fragments [3,7].

It is worthwhile noting the different roles played by neutron and  $\gamma$ -ray emission in fragment de-excitation. At scission, the total available excitation energy is partitioned between the two fragments in the form of intrinsic energy, shape deformation, and collective motion [4]. Neutron and  $\gamma$ -ray emission takes place from fully accelerated fragments, giving enough time for the nuclear deformation to relax into excitation energy. Neutrons, due to their binding energies, dissipate the largest portion of the fragment intrinsic energy, i.e., the energy not stored in collective rotational motion of nucleons. STAT  $\gamma$  rays dissipate the remaining intrinsic excitation energy until a rotational band is reached. DISC  $\gamma$  rays dissipate the remaining rotational energy and angular momentum. The emission of DISC  $\gamma$  rays is regulated most strongly by the feeding of rotational band levels, which in turn depends on the initial angular momenta of the fragment.

In the remainder of this section we will investigate the sources of possible neutron- $\gamma$  correlations. Positive neutron- $\gamma$  multiplicity correlations, in the present context, indicate that

the emission of each neutron makes it more likely to emit a  $\gamma$  ray. Negative correlations represent the opposite.

### B. Decay competition

The most direct source of correlations is the competition between neutron and  $\gamma$ -ray emission. In theory, this competition could result in very strong negative correlations between the neutron and  $\gamma$ -ray multiplicity. In practice, the two decay modes can be treated as independent apart from a narrow intrinsic energy range near the neutron separation energy [12,13]. The  $\gamma$  rays competing with the neutrons are STAT. Furthermore, because the fragments are less excited close to the neutron separation energy [14], we expect these negative correlations to appear at low neutron energies.

### C. Resource competition

Another significant source of neutron- $\gamma$  competition is that introduced by the finite excitation energy and angular momentum of the fragments. In fact, given the same excitation energy  $E^*$ , a fragment that dissipates more of its intrinsic energy through neutron evaporation will have less energy to dissipate through STAT  $\gamma$ -ray emission. The competition over the intrinsic energy of the fragments would result in overall negative correlations between neutrons and STAT  $\gamma$  rays.

Competition related to the fragment angular momentum  $J$  are more complicated, given the vector nature of the angular momentum. If neutron emission is found to remove significant quantities of angular momentum, we expect negative correlations between neutrons and DISC  $\gamma$  rays, since these are the  $\gamma$  rays mostly affected by the angular momenta of the fragments.

### D. Excitation energy and angular momentum

Correlations between neutrons and  $\gamma$  rays are expected if their emission depends on the same fragment properties. For example, we know that more energetic fission fragments will emit more energetic neutrons and STAT  $\gamma$  rays. Therefore we expect the spectra of neutrons and  $\gamma$  rays to receive contributions from their shared dependence on the fragment temperature [14].

The interesting and still unclear mechanism for angular momentum generation [2,15–18] can lead to correlated behavior in neutron- $\gamma$  emission. In fact, the intrinsic excitation energy is strongly linked to the neutron multiplicity [19], while the emission of DISC  $\gamma$  rays is regulated by the angular momentum [3,20]. Thus, if  $E^*$  and  $J$  are positively correlated, i.e., positive spin-energy correlations, as phenomenological and theoretical models predict [15,21,22], we also expect positive correlations between neutrons and DISC  $\gamma$  rays.

These correlations will be especially important in this work, since DISC  $\gamma$  rays have similar energies for many different probable fragments in fission, and can thus give rise to correlated structure. Experimentally, spin-energy correlations have not been conclusively proven. In fact their existence has been disputed by some [2,7], and supported by others [3,23]. See also Refs. [24–26]. Clearly, more experimental evidence regarding possible spin-energy correlations is needed.

TABLE I. Summary of the expected sources of neutron- $\gamma$  correlations.

Source	Sign of correlation	$\gamma$ type	Interfragment
Decay competition	Negative	STAT	No
Energy competition	Negative	STAT	No
Angular momentum competition	Negative	DISC	No
Fragment temperature	Overall neutral	STAT	Yes
Spin-Energy correlation	Positive	DISC	Yes

We note that  $\gamma$ -ray emission is correlated with the properties of the post-evaporation fission fragments. Therefore, the energy-spin correlations can be counterbalanced by the dissipation of the fragment energy and angular momentum during neutron emission.

### E. Interfragment correlations

While all of the sources of correlations discussed above are related to neutrons and  $\gamma$  rays from the same fragment, it is also possible to have correlations between emissions from opposite fragments. The strongest source of interfragment correlations are those related to the initial excitation energy and angular momentum of the fragments. If the fragments are assumed to have strongly correlated initial conditions, we expect the correlations between neutrons and  $\gamma$  rays originating from opposite fragments (interfragment) to be of the same order of magnitude as those between particles originating in the same fragment (intrafragment).

Because interfragment correlations do not suffer from internal decay competition or resource competition, we expect interfragment correlations to lack negative sources. Stated in an equivalent way, we expect interfragment correlations to be positive overall.

A noteworthy special case is mentioned here. If the initial fragment conditions are strongly correlated to one another but one of the fragments emits significantly fewer neutrons than the other, we expect interfragment correlations to be large. In fact, the angular momentum of the fragment emitting fewer neutrons would be less changed by neutron emission.

### F. Summary

We summarize the discussion of the possible origins of neutron- $\gamma$  correlations in Table I. For each source discussed, we specify whether we expect it to be introducing positive or negative correlations. We also distinguish, in the  $\gamma$ -type column, whether the correlations arise between neutrons and STAT  $\gamma$  rays or DISC  $\gamma$  rays. Lastly, we indicate whether these correlations can also arise from interfragment correlations.

## III. ANALYSIS

Having discussed why and where we expect to see correlations, we need to quantify their magnitude. In this section we

discuss a new type of statistical analysis of radiation data, the normalized differential multiplicity covariance.

### A. Covariance

Let us define the event-by-event neutron and  $\gamma$  multiplicities,  $N_n$  and  $N_\gamma$ . We investigate the correlations in the neutron- $\gamma$  emission by analyzing the multiplicity covariance  $\text{cov}(N_n, N_\gamma)$ . This quantity describes the linear correlations in the event-by-event fluctuations of the neutron and  $\gamma$  multiplicities with respect to the mean values. We have already shown in our previous study [10] that the neutron- $\gamma$  multiplicity covariance is negative. Decay competition has a negligible effect on the correlations integrated over all energies. Using Table I, we conclude that energy and angular momentum competition dominate over the other sources of correlations. To investigate the other sources, we analyze the dependence of the neutron- $\gamma$  covariance on the energies of the outgoing particles.

### B. Differentials

The energy-dependent covariance is introduced as the covariance between the neutron and  $\gamma$ -ray event-by-event spectra,

$$\text{cov}\left(\frac{dN_n}{dE_n}, \frac{dN_\gamma}{dE_\gamma}\right) = \frac{\partial^2 \text{cov}(N_n, N_\gamma)}{\partial E_n \partial E_\gamma}, \quad (1)$$

where  $E_n$  and  $E_\gamma$  are the neutron and  $\gamma$ -ray energies. The arguments of the covariance in the left-hand side of Eq. (1) are the event-by-event multiplicities differentiated by spectra, i.e., the number of particles emitted with a specified energy, listed for each fission event. The right-hand side of Eq. (1) then follows from the bilinearity of the covariance operator. The energy-differentiated covariance is then interpreted as the correlations between neutron and  $\gamma$  rays multiplicities, if only neutrons and  $\gamma$  rays of energies  $E_n$  and  $E_\gamma$  are counted. The differentiated covariance allows us to investigate how the emission of neutrons of a specified energy affects the emission of  $\gamma$  rays with another specified energy. For sufficiently narrow energy bins, the event-by-event multiplicity in each bin also tends to zero. For sufficiently small multiplicities, the correlations approach linearity and are described appropriately by the covariance.

### C. Covariance scaling

While the differential covariance describes the correlations between neutrons and  $\gamma$  rays, it also scales with the multiplicity in each energy bin. To compare the strength of the correlations across energies, we normalize the covariance by the independent spectra, i.e.,

$$C_{E_n, E_\gamma} = \frac{\partial^2 \text{cov}(N_n, N_\gamma)}{\partial E_n \partial E_\gamma} \left( \frac{d\langle N_n \rangle}{dE_n} \frac{d\langle N_\gamma \rangle}{dE_\gamma} \right)^{-1}. \quad (2)$$

With this choice of normalization,  $C_{E_n, E_\gamma}$  satisfies

$$C_{E_n, E_\gamma} \geq -1, \quad (3)$$

where the equality holds only in the case where the emission of a neutron of energy  $E_n$  completely precludes the emission of a  $\gamma$  ray of energy  $E_\gamma$ , and vice versa.

## IV. EXPERIMENT

### A. Experiment

We analyze the data of Marcath *et al.* [27] collected using the Chi-Nu array at the Los Alamos neutron science center (LANSCE). We have analyzed  $1.7 \times 10^{10}$   $^{252}\text{Cf}$  spontaneous fission events, each tagged by an ionization chamber fabricated at Oak Ridge National Laboratory [28]. Due to hardware limitations, only 42 of the 54 EJ-309 organic scintillation detectors were active during the measurement. Each detector was placed at a distance of approximately 1 m from the fission source. Coincidences between the EJ-309 detectors and the fission chamber are employed to measure the neutron and  $\gamma$ -ray multiplicities,  $D_n$  and  $D_\gamma$ , respectively, detected in each event. For more information on this experiment, see Refs. [10,27,29].

### B. Simulation and response

We performed a high-fidelity simulation of the system response using MCNPX-POLIMI [30,31], a Monte Carlo based radiation transport code. In the simulation, the response of each detector is individually modeled, taking into account any differences in distance to source, light output, and calibration. We introduce a small perturbation in the light outputs and the array geometry in the simulations to better reproduce the reference MCNPX-POLIMI neutron spectrum, the Watt spectrum, after radiation transport. The parameters of the light output response for each detector, modeled analytically as exponential functions [32], are slightly perturbed from the literature values to better fit the reference spectrum. Clearly, the unfolding procedure is systematically biased to reproduce the known  $^{252}\text{Cf}$ (sf) neutron spectrum. No corrections are applied to reproduce the  $\gamma$ -ray spectrum. The analysis of the simulated system response is presented in Fig. 2. The absolute detection efficiencies,  $\epsilon_n$  and  $\epsilon_\gamma$ , are not uniform across the emitted particle spectra.

### C. Unfolding matrices

In experiment, we do not have access to the emitted multiplicities,  $N_n$  and  $N_\gamma$ , or the emitted neutron and  $\gamma$ -ray energies  $E_n$  and  $E_\gamma$ . Rather, we have access to detected multiplicities  $D_n$  and  $D_\gamma$ , differentiated with respect to time of flight energy  $T_n$  for neutrons, and energy deposited by  $\gamma$  rays  $F_\gamma$ . Due to the large distance between detectors and source, time of flight leads to accurate assignment of the energy up to  $E_n \approx 7$  MeV. However, because  $\gamma$  rays interact through Compton scattering with the liquid organic scintillator, only a fraction of the energy is deposited in each  $\gamma$ -ray interaction.

In our simulations, we calculate the matrix  $dE_n/dT_n$  describing, for each neutron emitted with energy  $E_n$ , the probability of assigning it an energy of  $T_n$ . Similarly, we calculate  $dE_\gamma/dF_\gamma$  for the probability of a  $\gamma$  ray of energy  $E_\gamma$  to deposit energy  $F_\gamma$ . Energy and time resolution, determined from the

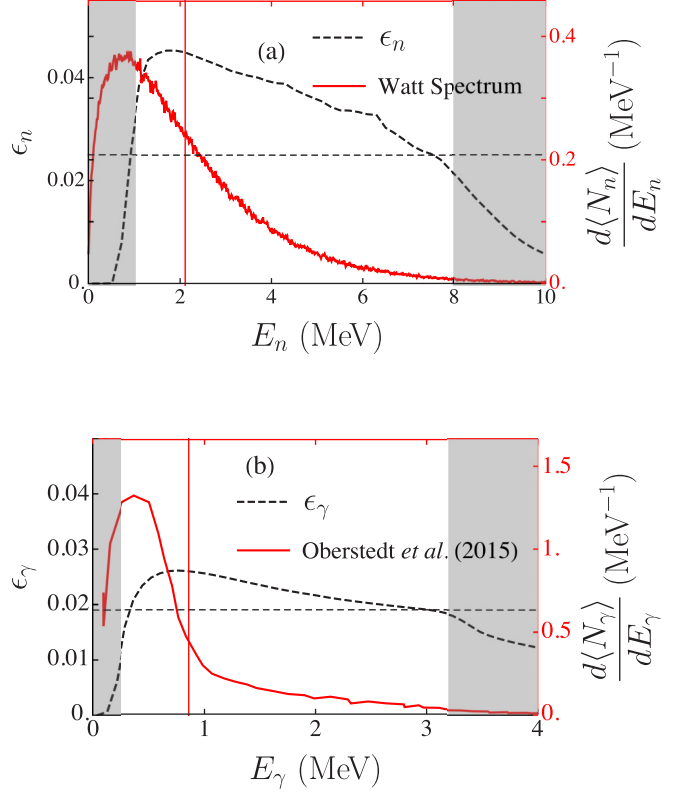


FIG. 2. Simulated energy response of the Chi-Nu array to (a) neutrons and (b)  $\gamma$  rays. The solid red line, referencing the right-hand axis, shows the evaluated neutron Watt spectrum included in the standard MCNPX-POLIMI californium source [30,31]. The  $\gamma$ -ray spectrum by Oberstedt *et al.* [33] is used here. The vertical red and horizontal dashed black lines represent respectively the mean emission energy and mean system efficiency. The grey bands indicate the regions outside the energy acceptance of the system.

experimental data, have been applied in simulation to smooth out all calculated results.

The unfolding of the measured neutron- $\gamma$  correlations and spectra is performed using the response matrices and the measured neutron- $\gamma$  correlations,

$$\frac{\partial^2 \text{cov}(N_n, N_\gamma)}{\partial E_n \partial E_\gamma} = \frac{\partial^2 \text{cov}(D_n, D_\gamma)}{\partial T_n \partial F_\gamma} \left( \epsilon_n \frac{dE_n}{dT_n} \right)^{-1} \left( \epsilon_\gamma \frac{dE_\gamma}{dF_\gamma} \right)^{-1}, \quad (4)$$

$$\frac{d\langle N_n \rangle}{dE_n} = \frac{d\langle D_n \rangle}{dT_n} \left( \epsilon_n \frac{dE_n}{dT_n} \right)^{-1}, \quad (5a)$$

$$\frac{d\langle N_\gamma \rangle}{dE_\gamma} = \frac{d\langle D_\gamma \rangle}{dF_\gamma} \left( \epsilon_\gamma \frac{dE_\gamma}{dF_\gamma} \right)^{-1}. \quad (5b)$$

### D. Regularization

To reduce the effects of noise in the unfolded distributions, we have applied Tikhonov regularization [34]. In this unfolding procedure, regularization parameters  $\alpha_n$  and  $\alpha_\gamma$  are introduced. The unfolding procedure is optimized and validated on the measured spectra, where we have determined the

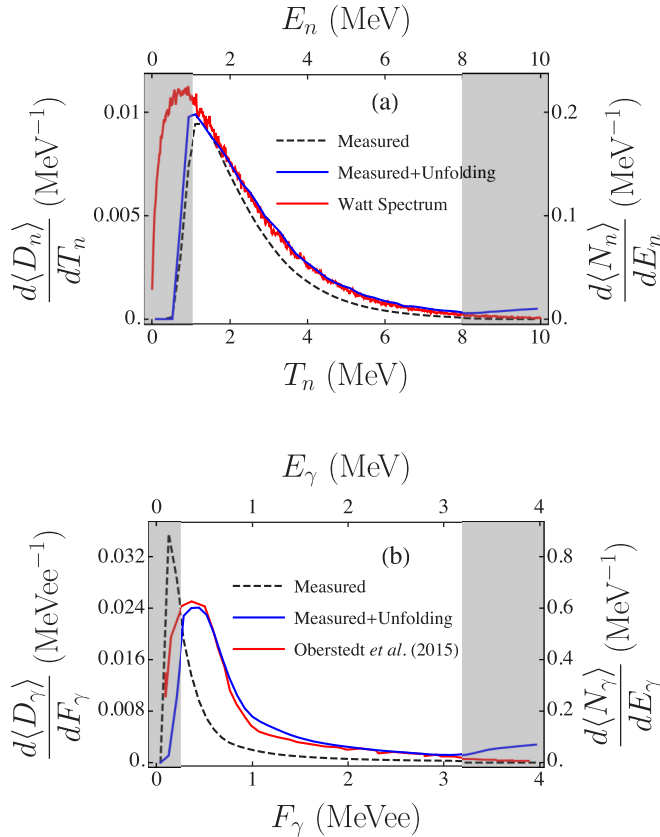


FIG. 3. Measured spectra and unfolded spectra after Tikhonov regularization. The same reference spectra given in Fig. 2 are also shown in red. The reference spectra are normalized to the area of the unfolded measurement in the acceptance region.

values of and uncertainties on  $\alpha_n$  and  $\alpha_\gamma$ . By comparison with the evaluated spectra, we have determined the effective acceptance regions in the unfolded distributions,  $1.2 \leq E_n \leq 8$  MeV and  $0.22 \leq E_\gamma \leq 3.2$  MeV. These acceptance regions, indicated by the areas between the shaded bands in Fig. 2, cover 66% and 78% of the neutron and  $\gamma$ -ray spectra, respectively. The results of the spectral unfolding procedure are shown in Fig. 3.

## V. RESULTS

The unfolding procedure introduced in the last section is applied to the experimental data. We have analyzed the data using energy bins of width 0.2 MeV for  $E_n$  and 0.08 MeV for  $E_\gamma$ . We present our experimental determination of  $C_{E_n, E_\gamma}$  in Fig. 4. We have included systematic errors associated with the unfolding by including experimental curves above and below the indicated fixed  $E_n$ . Systematic biases associated with background, particle misclassification, detector blinding, and inelastic  $\gamma$ -ray production are removed according to the procedure outlined in Ref. [10]. To facilitate the visualization of the data, we have included a horizontal dashed line indicating the average of the correlations across all  $E_n$  and  $E_\gamma$ .

We observe structure in the form of two enhancements at  $E_\gamma \approx 0.7$  and 1.2 MeV. A down slope develops at the low-

est energies, extending down to the rejection region at  $<0.3$  MeV. Higher-energy correlation enhancements start to appear with increasingly higher gates on neutron outgoing energies, notably at  $E_\gamma \approx 1.7$  MeV.

The experimental results are compared to the CGMF [5,35], FIFRELIN [11,26,36], and FREYA [37,38] model calculations. The release versions of CGMF and FREYA are used here. FIFRELIN results are shown for an energy independent (constant) and an energy dependent ( $E^*$ -dependent) model for the generation of angular momentum in the fragments [39]. A Gaussian smoothing informed by the energy resolution of the system is applied to all model calculations to be consistent with the data analysis. We note that the goal of the current analysis is not to compare any individual model calculations to the data, but rather to determine which features of the data differ from all the model calculations and can therefore offer insights into the fission mechanism. The feature of the correlations we focus on in this work are the correlations enhancements at  $E_\gamma = 0.7$  and 1.2 MeV.

### A. Enhanced correlation structure

The two correlation enhancements at 0.7 and 1.2 MeV appears to arise from DISC  $\gamma$  rays positively correlating to the emission of neutrons. The  $\gamma$  rays giving rise to these enhancements cannot be assigned to a single fragment level scheme, but are rather emergent behaviors from the combination of many transitions of similar energies. We note that much more work, both experimental and theoretical, is needed in order to quantify the spin-energy correlations.

Using CGMF and FIFRELIN, we have determined that the enhancement at 1.2 MeV corresponds to transitions from quasi-spherical heavy fragments near  $^{132}\text{Sn}$ . The enhancement at 0.7 MeV receives contributions from both light and heavy fragments, and it is due to electric quadrupole Yrast transitions with initial spins  $4\hbar$ ,  $6\hbar$ , and  $8\hbar$ . The predicted valley at  $E_\gamma < 0.4$  MeV is due to competition between neutron emission and DISC  $\gamma$  rays.

The correlation enhancement at  $E_\gamma = 0.7$  MeV indicates the existence of positive spin-energy correlations. In fact, the emission of neutrons correlates strongly with the intrinsic excitation energy of the fragment. Enhancements at  $E_\gamma \approx 0.7$  MeV indicate that the high-spin,  $J \approx 4-8 \hbar$  rotational bands are more populated with each neutron emission. This hypothesis is confirmed by comparing FIFRELIN calculations performed with and without spin-energy coupling. In the calculations, both shown in Fig. 4, we have found that the amplitude of the enhancement is strengthened significantly when the spin-energy coupling is considered. We have not attempted to quantify the strength of the spin-energy correlations from the experimental data, but this could be pursued in future work. Qualitatively, we can say that the observation of the enhanced correlations indicates the presence of spin-energy correlations in the generation of angular momentum in fission fragments.

The enhanced correlations at  $E_\gamma = 1.2$  MeV reveals less about the spin-energy correlations and more about biasing of the sample. In fact, the main contributor to this

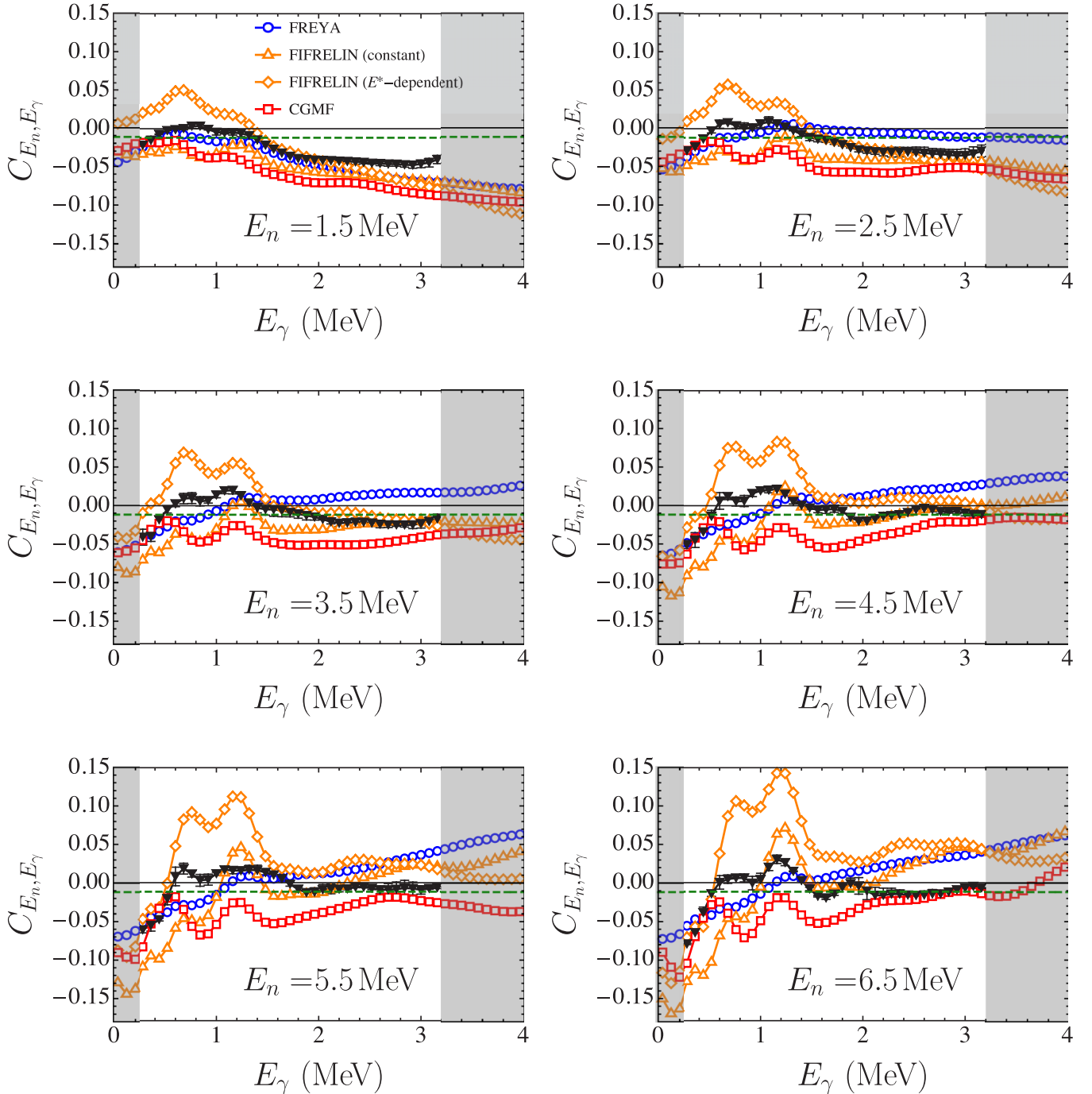


FIG. 4. Partial derivative analysis of the correlations. In each panel, the fixed neutron energy is indicated, and a green line represents the average of the experiment over all energies. The experimental data are shown in black, the error bars are given based on variations within neighboring  $E_n$  slices.

enhancement are low-spin transitions in the spherical fragment region. We note that neutron outgoing energies from near-symmetric fissions are generally higher than for the most probable splits [19]. The observation of high-energy neutrons in the laboratory frame thus biases the fission sample more strongly towards symmetric fission, and is thus positively correlated with high-energy DISC  $\gamma$ -ray emission.

## B. Other features

Two other notable features of the energy dependent correlations are their behaviors at the higher and lower end of the  $\gamma$ -ray spectrum. At high  $E_\gamma$ , the correlations are most representative of STAT emission, since these  $\gamma$  rays have a harder spectrum than those from DISC emission. In the calculations, we find that the intrafragment contributions to

the correlations involving STAT  $\gamma$  rays are predominantly negative. Therefore, we might interpret positive correlations at high  $E_n$  and  $E_\gamma$  as originating from interfragment correlations, and thus conclude from the experiment that interfragment correlations are not as strong as intrafragment correlations. This in turn would lead to the conclusion that the initial states of the fragments, specifically the intrinsic excitation energy, between the two fragments, are not strongly correlated.

Several problems exist with the above conclusion, which is premature at this stage, and will need to be investigated further. First of all, as mentioned for the enhancement at 1.2 MeV, gating on higher neutron energies does not only bias towards higher energy fragments, but also towards symmetric fission. Therefore, the correlations shown here are systematically biased by this selection. Second, in the calculations, we find that one of the largest sources of positive correlations in the high  $E_\gamma$  region are continuum-discrete transitions. Because these effects cannot be disentangled from the interfragment correlations, we do not attempt to draw conclusions based on this region.

At low  $E_\gamma$ , the correlations in the data are more negative than the average. The models predict this feature to originate from inter-fragment correlations, specifically between neutrons from the light fragment and DISC  $\gamma$  rays from the heavy fragment.

## VI. CONCLUSION

We have presented an investigation of the neutron- $\gamma$  correlations in  $^{252}\text{Cf}(\text{sf})$ . The first result of this study is the development and application of the normalized differential multiplicity covariance, a powerful tool in the analysis of radiation correlations. We have analyzed the correlations between neutrons and  $\gamma$  rays using the normalized differential multiplicity covariance. This analysis yielded previously unobserved structure in the neutron- $\gamma$  correlations. Specifically, we have presented experimental evidence of enhancements in neutron- $\gamma$  correlations around the  $\gamma$ -ray energies of 0.7 and 1.2 MeV. We have compared the experimental data to model

calculations, to determine the physical origins of the observed structure. The appearance of enhancements in the correlations can likely be explained by the correlations between excitation energy and angular momentum. Further theoretical and experimental studies will be needed to quantify the strength of these correlations.

An experiment involving event-by-event neutron- $\gamma$  correlations in coincidence with a fission fragment detector capable of measuring masses and kinetic energies is being planned. Such an experiment would further our understanding of energy and angular momentum correlations in fission and shed light on the decay competition of neutrons and  $\gamma$  rays near the neutron separation energy. Furthermore, there still remains significant disagreement in the literature about correlations between neutron- $\gamma$  competition and fragment properties. The planned experiment will investigate these correlations, perhaps leading to a reconciliation of previous results.

## ACKNOWLEDGMENTS

S.M. thanks the experimental group at LANSCE-LANL and M. J. Marcatch for sharing the experimental data used in this analysis. This work was in part supported by the Office of Defense Nuclear Nonproliferation Research & Development (DNN R&D), National Nuclear Security Administration, US Department of Energy. This research was funded in part by the Consortium for Verification Technology under Department of Energy National Nuclear Security Administration Award No. DE-NA0002534. The work of V.A.P. was performed under the auspices of UT-Battelle, LLC under Contract No. DE-AC05-00OR22725 with the U.S. Department of Energy. The work of P.T., A.E.L., and I.S. is carried out under the auspices of the National Nuclear Security Administration of the U.S. Department of Energy at Los Alamos National Laboratory under Contract No. 89233218CNA000001. The work of R.V. was performed under the auspices of the U.S. Department of Energy by Lawrence Livermore National Laboratory under Contract No. DE-AC52-07NA27344. J.R. acknowledges support from the Office of Nuclear Physics in the U.S. Department of Energy under Contract No. DE-AC02-05CH11231.

- [1] U. Brosa, S. Grossmann, and A. Müller, Nuclear scission, *Phys. Rep.* **197**, 167 (1990).
- [2] J. B. Wilhelmy, E. Cheifetz, R. C. Jared, S. G. Thompson, H. R. Bowman, and J. O. Rasmussen, Angular momentum of primary products formed in the spontaneous fission of  $^{252}\text{Cf}$ , *Phys. Rev. C* **5**, 2041 (1972).
- [3] H. Nifenecker, C. Signarbieux, M. Ribrag, J. Poitou, and J. Matuszek, Gamma-neutron competition in the de-excitation mechanism of the fission fragments of  $^{252}\text{Cf}$ , *Nucl. Phys. A* **189**, 285 (1972).
- [4] K. H. Schmidt and B. Jurado, Final excitation energy of fission fragments, *Phys. Rev. C* **83**, 061601(R) (2011).
- [5] P. Talou, R. Vogt, J. Randrup, M. E. Rising, S. A. Pozzi, J. Verbeke, M. T. Andrews, S. D. Clarke, P. Jaffke, M. Jandel, T. Kawano, M. J. Marcatch, K. Meierbachtol, L. Nakae, G. Rusev, A. Sood, I. Stetcu, and C. Walker, Correlated prompt fission data in transport simulations, *Eur. Phys. J. A* **54**, 9 (2018).
- [6] M. M. Hoffman, Directional correlation of fission fragments and prompt gamma rays associated with thermal neutron fission, *Phys. Rev.* **133**, B714 (1964).
- [7] R. Schmid-Fabian, Investigation of the spontaneous fission of Cf-252 at the heidelberg-darmstadt crystal-ball-spectrometer, Ph.D. thesis, University of Heidelberg, 1988.
- [8] U. Brosa, Sawtooth curve of neutron multiplicity, *Phys. Rev. C* **32**, 1438 (1985).
- [9] C. Signarbieux, J. Poitou, M. Ribrag, and J. Matuszek, Correlation entre les energies d'excitation des deux fragments complementaires dans la fission spontanee de  $^{252}\text{Cf}$ , *Phys. Lett. B* **39**, 503 (1972).
- [10] S. Marin, V. A. Protopopescu, R. Vogt, M. J. Marcatch, S. Okar, M. Y. Hua, P. Talou, P. F. Schuster, S. D. Clarke, and S. A.



- Pozzi, Event-by-event neutron–photon multiplicity correlations in  $^{252}\text{Cf}(\text{sf})$ , *Nucl. Instrum. Methods Phys. Res. A* **968**, 163907 (2020).
- [11] O. Litaize and O. Serot, Investigation of phenomenological models for the Monte Carlo simulation of the prompt fission neutron and  $\gamma$  emission, *Phys. Rev. C* **82**, 054616 (2010).
- [12] T. D. Thomas and J. R. Grover, Angular momentum effects in the  $\gamma$ -ray de-excitation of fission fragments, *Phys. Rev.* **159**, 980 (1967).
- [13] A. Spyrou, S. N. Liddick, F. Naqvi, B. P. Crider, A. C. Dombos, D. L. Bleuel, B. A. Brown, A. Couture, L. Crespo Campo, M. Guttormsen, A. C. Larsen, R. Lewis, P. Möller, S. Mosby, M. R. Mumpower, G. Perdikakis, C. J. Prokop, T. Renström, S. Siem, S. J. Quinn, and S. Valenta, Strong Neutron- $\gamma$  Competition Above the Neutron Threshold in the Decay of  $^{70}\text{Co}$ , *Phys. Rev. Lett.* **117**, 142701 (2016).
- [14] J. M. Blatt and V. F. Weisskopf, *Theoretical Nuclear Physics*, Dover Books on Physics Series (Dover Publications, Mineola, New York, 1991).
- [15] L. Bonneau, P. Quentin, and I. N. Mikhailov, Scission configurations and their implication in fission-fragment angular momenta, *Phys. Rev. C* **75**, 064313 (2007).
- [16] V. Rakopoulos, M. Lantz, A. Solders, A. Al-Adili, A. Mattera, L. Canete, T. Eronen, D. Gorelov, A. Jokinen, A. Kankainen, V. S. Kolhinen, I. D. Moore, D. A. Nesterenko, H. Penttilä, I. Pohjalainen, S. Rinta-Antila, V. Simutkin, M. Vilén, A. Voss, and S. Pomp, First isomeric yield ratio measurements by direct ion counting and implications for the angular momentum of the primary fission fragments, *Phys. Rev. C* **98**, 024612 (2018).
- [17] J. N. Wilson, D. Thisse, M. Lebois, N. Jovančević, D. Gjestvang, R. Canavan, M. Rudigier, D. Étasse, R.-B. Gerst, L. Gaodefroy, E. Adamska, P. Adsley, A. Algora, M. Babo, K. Belvedere, J. Benito, G. Benzoni, A. Blazhev, A. Boso, S. Bottoni, M. Bunce, R. Chakma, N. Cieplicka-Oryńczak, S. Courtin, M. L. Cortés, P. Davies, C. Delafosse, M. Fallot, B. Fornal, L. Fraile, A. Gottardo, V. Guadilla, G. Häfner, K. Hauschild, M. Heine, C. Henrich, I. Homm, F. Ibrahim, E. W. Iskra, P. Ivanov, S. Jazrawi, A. Korgul, P. Koseoglou, T. Kröll, T. Kurtukian-Nieto, L. Le Meur, S. Leoni, J. Ljungvall, A. Lopez-Martens, R. Lozeva, I. Matea, K. Miernik, J. Nemer, S. Oberstedt, W. Paulsen, M. Piersa, Y. Popovitch, C. Porzio, L. Qi, D. Ralet, P. H. Regan, K. Rezynekina, V. Sánchez-Tembleque, S. Siem, C. Schmitt, P.-A. Söderström, C. Sürder, G. Tocabens, V. Vedia, D. Verney, N. Warr, B. Wasilewska, J. Wiederhold, M. Yavahchova, F. Zeiser, and S. Ziliani, Angular momentum generation in nuclear fission, *Nature* **590**, 566 (2021).
- [18] J. Randrup and R. Vogt, Generation of fragment angular momentum in fission, [arXiv:2103.14778](https://arxiv.org/abs/2103.14778) [nucl-th] (2021).
- [19] A. Göök, F.-J. Hamsch, and M. Vidali, Prompt neutron multiplicity in correlation with fragments from spontaneous fission of  $^{252}\text{Cf}(\text{sf})$ , *Phys. Rev. C* **90**, 064611 (2014).
- [20] R. Vogt and J. Randrup, Angular momentum effects in fission, *Phys. Rev. C* **103**, 014610 (2021).
- [21] G. F. Bertsch, W. Loveland, W. Nazarewicz, and P. Talou, Benchmarking nuclear fission theory, *J. Phys. G: Nucl. Part. Phys.* **42**, 077001 (2015).
- [22] J. Randrup and R. Vogt, Refined treatment of angular momentum in the event-by-event fission model FREYA, *Phys. Rev. C* **89**, 044601 (2014).
- [23] A. Chebboubi, G. Kessedjian, O. Litaize, O. Serot, H. Faust, D. Bernard, A. Blanc, U. Köster, O. Méplan, P. Mutti, and C. Sage, Kinetic energy dependence of fission fragment isomeric ratios for spherical nuclei  $^{132}\text{Sn}$ , *Phys. Lett. B* **775**, 190 (2017).
- [24] J. Fréhaut, A. Bertin, and R. Bois, Mesure de  $\bar{\nu}$  et  $\bar{E}_\gamma$  pour la fission de  $^{232}\text{Th}$ ,  $^{235}\text{U}$  et  $^{237}\text{Np}$  induite par des neutrons d'énergie comprise entre 1 et 15 Mev, in *Nuclear Data for Science and Technology*, edited by K. H. Böckhoff (Springer Netherlands, Dordrecht, 1983), pp. 78–81.
- [25] T. Wang, G. Li, L. Zhu, Q. Meng, L. Wang, H. Han, W. Zhang, H. Xia, L. Hou, R. Vogt, and J. Randrup, Correlations of neutron multiplicity and  $\gamma$ -ray multiplicity with fragment mass and total kinetic energy in spontaneous fission of  $^{252}\text{Cf}$ , *Phys. Rev. C* **93**, 014606 (2016).
- [26] L. Thulliez, O. Litaize, O. Serot, and A. Chebboubi, Neutron and  $\gamma$  multiplicities as a function of incident neutron energy for the  $^{237}\text{Np}(\text{n},\text{f})$  reaction, *Phys. Rev. C* **100**, 044616 (2019).
- [27] M. J. Marcatch, R. C. Haight, R. Vogt, M. Devlin, P. Talou, I. Stetcu, J. Randrup, P. F. Schuster, S. D. Clarke, and S. A. Pozzi, Measured and simulated  $^{252}\text{Cf}(\text{sf})$  prompt neutron-photon competition, *Phys. Rev. C* **97**, 044622 (2018).
- [28] L. E. Kirsch, M. Devlin, S. Mosby, and J. Gomez, A new measurement of the  $^6\text{Li}(\text{n},\alpha)\text{t}$  cross section at Mev energies using a  $^{252}\text{Cf}$  fission chamber and  $^6\text{Li}$  scintillators, *Nucl. Instrum. Methods Phys. Res. A* **874**, 57 (2017).
- [29] P. F. Schuster, M. J. Marcatch, S. Marin, S. D. Clarke, M. Devlin, R. C. Haight, R. Vogt, P. Talou, I. Stetcu, T. Kawano, J. Randrup, and S. A. Pozzi, High resolution measurement of tagged two-neutron energy and angle correlations in  $^{252}\text{Cf}(\text{sf})$ , *Phys. Rev. C* **100**, 014605 (2019).
- [30] S. A. Pozzi, E. Padovani, and M. Marseguerra, MCNP-PoliMi: A monte-carlo code for correlation measurements, *Nucl. Instrum. Methods Phys. Res. A* **513**, 550 (2003).
- [31] S. A. Pozzi, S. D. Clarke, W. J. Walsh, E. C. Miller, J. L. Dolan, M. Flaska, B. M. Wieger, A. Enqvist, E. Padovani, J. K. Mattingly, D. L. Chichester, and P. Peerani, MCNPX-PoliMi for nuclear nonproliferation applications, *Nucl. Instrum. Methods Phys. Res. A* **694**, 119 (2012).
- [32] M. A. Norsworthy, A. Poitrasson-Rivière, M. L. Ruch, S. D. Clarke, and S. A. Pozzi, Evaluation of neutron light output response functions in EJ-309 organic scintillators, *Nucl. Instrum. Methods Phys. Res. A* **842**, 20 (2017).
- [33] A. Oberstedt, R. Billnert, F.-J. Hamsch, and S. Oberstedt, Impact of low-energy photons on the characteristics of prompt fission  $\gamma$ -ray spectra, *Phys. Rev. C* **92**, 014618 (2015).
- [34] V. A. Morozov, in *Methods for Solving Incorrectly Posed Problems*, edited by Z. Nashed (Springer-Verlag, New York, 1984).
- [35] P. Talou, I. Stetcu, P. Jaffke, M. E. Rising, A. E. Lovell, and T. Kawano, Fission fragment decay simulations with the CGMF code, *Comput. Phys. Commun.* **269**, 108087 (2021).
- [36] O. Litaize, O. Serot, and L. Berge, Fission modelling with FIFRELIN, *Eur. Phys. J. A* **51**, 177 (2015).
- [37] J. Randrup and R. Vogt, Calculation of fission observables through event-by-event simulation, *Phys. Rev. C* **80**, 024601 (2009).
- [38] J. M. Verbeke, J. Randrup, and R. Vogt, Fission reaction event yield algorithm FREYA 2.0.2, *Comput. Phys. Commun.* **222**, 263 (2018).
- [39] L. Thulliez, O. Litaize, and O. Serot, Sensitivity studies of spin cut-off models on fission fragment observables, *EPJ Web Conf.* **111**, 10003 (2016).